Egypt. J. Chem. **Vol. 67**, No. 10 pp. 619- 627 (2024)

Egyptian Journal of Chemistry

http://ejchem.journals.ekb.eg/

Bioactive constituents from two *Aspergillus* sp. extracts and Evaluation of their ADME-related physicochemical properties

Sally El Said Abo Halawa Abdelrahman[1], Mosad A. Ghareeb[2,*], Engy Mohsen[1,*], Ahmed A. Hamed[3], Seham El Hawary[1]

[1]Pharmacognosy *Department, Faculty of Pharmacy, Cairo University, Egypt*
[2]*Medicinal Chemistry Department, Theodor Bilharz Research Institute, Kornish El-Nile, Warrak El-Hadar, Imbaba, Giza 12411, Egypt*
[3]*Microbial Chemistry* Department, National Research Centre, 33 El-Buhouth Street, Dokki, Giza 12622, Egypt

Abstract
Marin habitats are rich of bioactive compounds with unique structures and biological activities. In this research two fungal strains were isolated from the Red Sea in Egypt coded as *Aspergillus sp.* SA17 and *Aspergillus sp.* SA18. Four compounds were structurally elucidated as 2-pentyl tetrahydrofuran (C1), 2-pentyl-3,4-dihydrofuran (C2), (Z)-2-(hepta-1-en-1-yl)tetrahydrofuran (C3), and 2-(3-methyl butane-1-en-1-yl) tetrahydrofuran (C4). The antimicrobial results showed that, the SA17 crude extract has significant efficacy, particularly against *S. aureus* and *Candida albicans*, with modest impact on *A. niger* and limited effectiveness against *E. coli*. On the other hand, C2 from SA17 demonstrating significant activity against *E. coli*. The SA18 extract exhibit diminished antibacterial efficacy and a higher degree of selectivity. In addition, the inhibition of acetylcholinesterase (AChE) by crude and purified substances from fungal sources SA17 and SA18 was investigated at various doses. The SA17 crude extract has a moderate inhibition that is dependent on its concentration. However, its purified constituent C2 displays a potent inhibitory action which surpasses that of the crude extract. SA18's crude extract exhibits strong inhibition, whereas its refined component C4 has a moderate but significant impact. Both C1 from SA17 and C3 from SA18 do not contribute to the inhibition of AChE, highlighting the variety in the effectiveness of these compounds obtained from fungi. Furthermore, the most potent compound was selected and studied for its ADME-physicochemical studies. In the light of this study, we can conclude that, endophytic fungi are a potential source for bioactive metabolites with diverse medical applications.
Keywords: *Aspergillus sp.*; Antimicrobial, Acetylcholinesterase inhibition; Bioactive metabolites; ADME

1. Introduction

Fungi are important sources of a broad variety of secondary metabolites. They produce a diverse array of bioactive compounds, also called natural products, which serve as a source of inspiration for the design of novel drugs [1]. The relevance of fungal natural products is demonstrated by the frequency of drugs derived from them. For many years, fungi were isolated from their environment and cultivated to obtain the compound biosynthesis, to optimize it, and to sustain self-sufficiency for their biomass production [2]. Recently, the chemical investigation of endophytic fungi through fermentation has gained attractiveness as a clue U8to potentially novel secondary metabolites. Endophytic fungi are capable of producing the same metabolites encountered in their host plants, suggesting that they have the potential for synthesizing these compounds [3].

Endophytic fungi have the ability to tolerate the observed compounds as an adaptive strategy to avoid being recognized by the plant defense apparatus, or translocate compounds from the host plant to other counterparts, or even synthesize them de novo. However, culture-dependent studies have failed to document endophytic production, as endophytic fermentation by endophytic fungi completes earlier in the life of the plant, prior to germination or shortly thereafter, intracellularly during the germination phase in specific host tissue near the epidermal surface of the host seed or seedling root [4]. The success of fermentation studies on high-level production of the desired product depends on the best bioprocess conditions, optimization, and control of interactions between the useful endophytes and the host plant in

*Corresponding author: E-mail: m.ghareeb@tbri.gov.eg (Mosad A. Ghareeb)
Receive Date: 13 August 2024, Revise Date: 05 September 2024, Accept Date: 13 September 2024
DOI: 10.21608/ejchem.2024.311926.10187

order to obtain the compound in a high yield. These factors guarantee the minimal loss of bioactive molecules to account for the scalability and sustainability of production expenses, assurance of the highest purity of the desired product, while reducing quantities of additional compounds stated from any contaminants, thus enabling the commercial development of biotechnological projects [5].

Endophytic fungi have been defined as those that colonize the internal tissues of plants without causing any apparent symptoms of disease. They reside in inter- or intracellular spaces and are capable of expressing an ecologically diverse array of phenotypes that may confer benefit to the host. In this relationship, endophytic fungi are considered as latent mutualists that often serve a protective role for plants against environmental stressors such as herbivores, pests, and pathogens. One of the most recognized roles of endophytic fungi is that of biocontrol agents against herbivores and pathogens. The biocontrol of postharvest diseases caused by endophytic fungi is a booming area and food waste can be reduced by suppressing damage. However, the generic relationship derives from the ecological relationship among endophytic fungi and their hosts [6].

Over the years, various types of secondary metabolites from endophytic fungi have been shown to possess a wide array of biological activities, including antimicrobial, anticancer, antiviral, and antioxidant activities [7]. However, the most studied secondary metabolite classes of endophytic fungi are alkaloids, phenolic compounds, and terpenoids. Notably, the antimicrobial capabilities of fungal endophytes derive largely from their biosynthetic pathways that evolve as adaptations capability of fungal endophytes to produce antimicrobial compounds share similar patterns but lower abundance compared with transplants compared to leaf microbiome communities [8]. Despite the central importance of endophytic fungi to plant microbial communities, there is limited knowledge about how host and environmental factors shape the structure and function of endophytic communities. This aspect is increasingly important considering the role that endophytic fungal communities may play in conferring host resistance to emerging plant pathogens [9]. Therefore, the current study aims to Therefore, the current study aims to evaluate the antimicrobial and acetylcholinesterase activities of *Aspergillus sp.* extracts and to identify their chemical constituents followed by evaluation of their ADME-related physicochemical properties.

2. Materials and Methods

2.1. Sampling

Samples of marine sponges were obtained from Hurghada (27.2579° N, 33.8116° E), a seaside city well-known for its variety of marine environments. Divers with SCUBA diving training carried out the collection underwater, carefully identifying and gathering sponges from various substrates, such as seagrass and sponges, at each location. The samples were collected, given special codes, taken pictures of, and then placed in the Microbial Chemistry Department in Egypt [10,11].

2.2. Separating related fungi from sponge samples

The first step in isolating related fungi involved surface-sterilizing the gathered marine spong samples. To do this, the sponges were first cleaned with tap water and then subjected to a series of treatments, including 70% ethanol, sterile distilled water, 2% sodium hypochlorite, and repeated rinses with distilled water. After the sponge had been surface-sterilized, it was chopped into small pieces and placed on a potato dextrose agar (PDA) medium that had been enhanced with chloramphenicol and nalidixic acid to prevent the growth of bacteria. After that, the plates were incubated at 28 °C until fungal colonies started to form. The Microbial Chemistry Department of the National Research Centre selected individual fungal colonies, sub-cultured them multiple times to ensure purity, and kept them in glycerol stocks at −20 °C [1,12,13].

2.3. Genetic identification of selected fungi

To verify the identity of the two fungal isolates, the 18S rRNA sequencing was examined. After the fungus was grown for three days at 28 °C in a 250 mL Erlenmeyer flask with 50 mL of potato dextrose broth medium, the fungal DNA was extracted. Following incubation, the mycelia were removed, and the Qiagen DNeasy Mini Kit, USA, was used to extract the DNA. [14]. Two global primers, NS3 (5′-GCAAGTCTGGTGCCAGCAGCC amplification 3′) and NS4 (5′-CTTCCGTCAATTCCTTTAAG-3′), were used to amplify the 18S rRNA gene [15]. Following a 5-minute denaturation stage at 94 °C, there were The PCR profile consisted of 35 cycles at 94 °C for 30 s, 55 °C for 30 s, 72 °C for 90 s, and a 5-minute extended step at 72 °C. A 5-minute denaturation phase at 94 °C was then followed by 35 cycles of 30 seconds at 94 °C, 30 seconds at 55 °C, 90 seconds at 72 °C, and a 5-minute extended step at 72 °C. The PCR product was sequenced at the South Korean SolGent Company. To ascertain the degree of homogeneity with all deposited sequences found in the NCBI (National Centre for Biotechnology Information) database, the resulting sequence was subjected to BLAST analysis. The MEGA7 program created the evolutionary tree [16,17].

2.4. Fungal cultivation and large-scale production

The fungal isolates were cultured using 100 g of rice and 100 mL of artificial seawater (with the salinity reduced to 50%). The incubation process lasted for 15 days at 28 °C. The culture was extracted using ethyl acetate (EtOAc) after the incubation time. The crude extract was then created by drying the EtOAc extract in a vacuum [18].

2.5. Chromatographic investigation of the ethyl acetate fraction of SA17 & SA18

2.5.1. Thin-layer chromatography analysis

Slica gel GF_{254} plates were used for TLC analysis of the ethyl acetate fraction using a few milligrams diluted in methanol. Following heating and spraying with a vanillin-sulfuric acid spray reagent, the plates employing pet. ether: $CHCl_3$; 70:30; v/v as the mobile phase were air dried and visualized. The quantity, hue, and R_f values of the exposed spots are noted (Table 1).

Table 1: Results of TLC investigation of the ethyl acetate fraction of SA17 & SA18

TLC detected spots (Pet. ether: chloroform; 7:3; v/v)		Color after spraying with vanillin-H_2SO_4	
R_f SA17	R_f SA18	SA17	SA18
0.93 minor	0.81 major	Purple	Green
0.89 major	0.76 minor	Green	Pink
0.74 major	0.61 major	Pink	Yellow
0.69 major	0.55 minor	Purple	Yellow
0.62 minor	0.50 major	Yellow	Purple
0.57 major	0.43 minor	Green	Yellow
0.50 major	0.33 major	Pink	Yellow
0.33 minor	0.24 minor	Orange	Purple
0.29 minor	0.19 minor	Purple	Yellow
0.26 minor	0.14 minor	Yellow	Pink

2.5.2. Phytochemical investigations

The ethyl acetate (EtOAc) extract (1.49 g) from the fungal strains *Aspergillus* sp. SA17 was chromatographed on silica gel-60 utilizing chloroform as a gradient elution system (0-100). The similar fractions were combined together based on their pattern upon TLC (GF_{254} plates) eluted with (Pet. ether: chloroform 70:30; v/v), and vanillin/H_2SO_4 as spraying system. A major fraction (4–8) was collected and re-chromatographed over Sephadex LH-20 column (7gm, 10×1cm) eluted with chloroform: methanol (9:1; v/v), the resulting sub-fractions were collected together to afford a yellow amorphous powders referred to compound 17A (15 mg) and compound 17B (9 mg) (Flowchart 1). Similarly, the ethyl acetate (EtOAc) extract (1.95 g) from the fungal strains *Aspergillus* sp. SA18 was chromatographed on silica gel-60 utilizing chloroform as elution system (0-100).

The similar fractions were combined together based on their pattern upon TLC (GF_{254} plates) eluted with (Pet. ether: chloroform; 70:30; v/v), and vanillin/H_2SO_4 as spraying system. A major fraction (24-57) was eluted from the column using (Pet. ether: chloroform; 70:30; v/v). This fraction was re-chromatographed over Sephadex LH-20 column (7gm, 10×1cm) eluted with chloroform/methanol (9:1; v/v), the resulting sub-fractions were collected together to afford a yellow amorphous powders referred to compound 18A (7 mg) and compound 18B (5 mg) (Flowchart 1).

Flowchart 1: Chromatographic isolation of the ethyl acetate fractions from *Aspergillus* SA17 & SA18.

2.6. Antimicrobial examination

Using a 96-well polystyrene microplate experiment, the antibacterial activity of the fungal crude extracts was assessed against a variety of pathogens, including penicillin-resistant *E. coli* (ATCC 25922), *C. albicans* (ATCC 10233), *A. niger*, and *S. aureus* (ATCC 6538). Positive reference antibiotics were Nystatin (5 µg/mL)

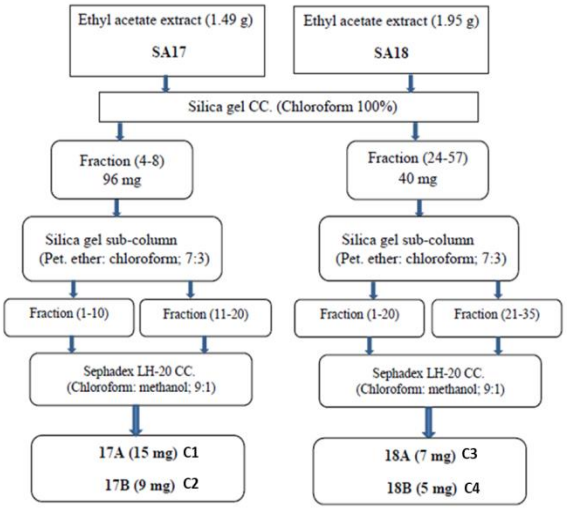

and Ciprofloxacin (10 µg/mL). The National Research Centre (NRC), Egypt's Culture Collection Centre (Microbial Chemistry Department) provided all test pathogens.

2.7. Assay for acetylcholinesterase inhibition efficacy

Using eight crude extracts, the inhibitory activity against acetylcholinesterase was investigated. An alteration was made to the Ingkaninan et al. approach in order to quantify enzymatic activity [20]. A 1 ml cuvette was used as a blank and included 500 µL of DTNB (3 mM), 100 µL of AChI (15 mM), 275 µL of Tris–HCl buffer (50 mM, pH 8), and 100 µL of sample at 10, 20, 40, 60, 80, and 100 µg mL^{-1}. Instead of using 25 µL of buffer, an enzyme solution containing 0.28 UmL^{-1} was utilized in the experiment. The statistics shown are the average of three replicates, and the

reaction was observed for five minutes at 405 nm. The use of erythrin hemi sulphate as a positive control and was tested at different concentrations than the samples. The concentrations of eserine tested were 0.01, 0.02, 0.04, and 0.08 μg mL^{-1} [21].

2.8. Statistical analysis

Results were analyzed statistically using the computerized program SPSS software, version "20" for windows. Data were represented as mean ± SE.

3. Results and Discussion

3.1. Separation of the fungal isolates from various marine specimens

The two fungal strains *Aspergillus* sp. SA17 and *Aspergillus* sp. SA18 were separated and cleaned from the gathered marine specimens. The morphological characteristics of the fungal colonies were used in their selection. The acquired strain was stored at 4 °C in the National Research Center's Microbial Chemistry Department in Egypt. Based on their physical traits, the isolated fungal isolates SA17 and SA18 were initially identified (REF).

3.2. Genetic identification of the two isolates

With reference to the initial assessment of the separated fungus, the two fungal strains were identified by means of 18S rRNA gene sequencing. Then, using the BLAST method to determine the symmetry record and statistical significance of the matches, the DNA of the fungal sample was extracted, amplified, and identified by comparing it with other known deposited genes in the GeneBank database (https://blast.ncbi.nlm.nih.gov/Blast.cgi, accessed on 1 February 2023). The results showed that the isolate's 18S rRNA gene configurations were similar, and that *Aspergillus* sp. exhibited 100% symmetry and deposited at GenBank as *Aspergillus sp.* SA17 (OP741150) and *Aspergillus sp.* SA18 (OP741189).

3.3. The bioactive substances' purification and structural clarification

Herein, we report the chromatographic isolation and purification of four compounds from the two fungal strain *Aspergillus* sp. SA17 and *Aspergillus* sp. SA18. The chemical structure of the pure isolates was established via using NMR spectroscopy (^{1}H, ^{13}C-NMR) (Fig. 1).

Compound 1: The ^{1}H-NMR (400 MHz, CD_3OD) spectrum of the compound displayed characteristic signals in the aliphatic region with chemical shift (δ) values of 0.91 (3H, t, *J* = 6.9, CH_3), 1.32-1.35 (10H, m, $(CH_2)_4CH_3$+$OCH_2(CH_2)_2$, 3.3 (4H, m, OCH_2+$OCH_2(CH_2)_2$, and 4.60 (1H, q, *J*= 7.1, $OCHCH_2$). The terahydrofuran skeleton was verified from ^{1}H-NMR spectrum of compound 1 which clearly indicated by the signals at δ 1.32-1.35 and 3.3 ppm for two CH_2 and an OCH_2, respectively in the tetrahydrofuran moiety [23-25]. The substitution at position 2 was concluded from the signals at δ 4.60 (1H, q, *J*= 7.1, $OCHCH_2$**)** [23,24,26]. The presence of side chain-(pentane) in the position 2 of tetrahydronfuran was deduced from a signal at δ 1.23-1.35 ppm (8H, m, $(CH_2)_4CH_3$) in addition to the methyl connected to a methylene carbon (CH_2Me) at the signal δ 0.91 ppm (3H, t, *J* = 6.9, CH_3). Therefore, compound 1 was finally identified as 2-pentyl tetrahydrofuran [23,24,26].

Compound 2: The ^{1}H-NMR (400 MHz, CD_3OD) spectrum of the compound displayed characteristic signals in the aliphatic region with chemical shift (δ) values of 0.90 (3H, t, *J* = 6.9, CH_3), 1.23–1.44 (8H, m, $(CH_2)_4CH_3$), 3.47 (1H, td, *J* = 7.9, 6.2, OCH_2), 4.22 (1H, td, *J* = 7.9, 6.2, OCH_2), 4.23 (1H, q, *J*= 7.1, OCHCH), 7.60 (1H, m, OCH_2CH), and 7.80 (1H, q, OCHCH). The 2,5 double bond in dihydrofuran skeleton was verified from ^{1}H-NMR spectrum of compound 2 which clearly indicated by the two signals at δ 3.47 and 4.22 ppm assignable to (1H,OCH_2) and the other (1H, OCH_2) in addition to the signals at δ 7.60 and7.80 ppm assignable to CH=CH in the 3,4- dihydrofuran moiety [24]. The substitution at position 2 was concluded from the signal at δ 4.23 (1H, q, *J*= 7.1, OCHCH) [24,25]. The presence of side chain-(pentane) in the position 2 of 3,4-dihydronfuran was deduced from a signal at δ 1.23–1.44 ppm (8H, m, $(CH_2)_4CH_3$) in addition to the methyl connected to a methylene carbon (CH_2Me) at the signal δ 0.90 ppm (3H, t, *J* = 6.9, CH_3). Therefore, compound 2 was finally identified as 2-pentyl-3,4-dihydrofuran [23,24].

Compound 3: The ^{1}H-NMR (400 MHz, CD_3OD) spectrum of the compound displayed characteristic signals in the aliphatic region with chemical shift (δ) values of 0.89 (3H, t, *J* = 6.9, CH_3),1.04 (1H, dq, $OCH_2(CH_2)_2$), 1.25-1.40 (6H, m, $(CH_2)_3CH_3$), 1.62-1.79 (5H, m, $CH=CHCH_2$ + $OCH_2(CH_2)_2$), 3.33 (2H, m, OCH_2), 4.03-4.1 (1H, q, *J* = 7.1, OCHCH=CH), 5.31 (1H, dd, *J* = 15.3, 7.2, OCHCH=CH), and 5.56 (1H, dt, *J* = 15.3, 6.7, OCHCH=CH). The terahydrofuran skeleton was verified from ^{1}H-NMR spectrum of compound 3 which clearly indicated by signals at δ 1.04 and 1.25-1.40 ppm for two CH_2 in addition to the signal at δ 3.33 for OCH_2 in the tetrahydrofuran moiety (1,2,3). The substitution at position 2 was concluded from the signal at δ 4.03-4.1 ppm (1H, $OCHCH_2$). The presence of side chain hepta-1-en-1-yl in the position 2 for tetrahydronfuran moiety was confirmed by two signals at δ 5.31 and 5.56 ppm assignable to two protons one proton for each CH=CH in addition to a signal at δ 1.62-1.79 assignable to the CH_2 in position 3ˈ for hepta-1-en-1-yl together with the signal at δ 1.25-1.40 ppm (6H)

assignable to the remaining three CH_2 in the side chain [23]. Therefore, compound 3 was finally identified as (*Z*)-2-(hepta-1-en-1-yl)tetrahydrofuran [23].

Compound 4: The ^{1}H-NMR (400 MHz, CD_3OD) spectrum of the compound displayed characteristic signals in the aliphatic region with chemical shift (δ) values of 1.46 (1H, dq, *J* = 11.8, 8.2, $OCH_2(CH_2)_2$),1.62 (3H, d, C**H**$_3$), 1.64 (3H, d, C**H**$_3$) 1.91-2.07(2H, m, $OCH_2(CH_2)_2$), 2.37 (1H, q, *J* = 6.9, OCH_2 $(CH_2)_2$), 2.43 (1H, m, OCHCH=CHCH), 3.32-3.67 (2H, td, *J* = 7.9, 6.2, OCH_2), 3.9 (1H, td, $OCHCH=CHCHMe_2$), 5.37 (1H, dd, *J* = 15.5, 7.2, OCHCH=CH), 5.43 (1H, dd, *J* = 15.5, 6.6, OCHCH=CH). Also, in ^{13}C-NMR (100 MHz, CD_3OD), it showed set of resonances: δ 16.4, 29.3, 36.7, 37.9, 38.0, 72.9, 73.4, 132.7, and 136.1 ppm. The terahydrofuran skeleton was verified from ^{1}H-NMR spectrum of 18-B which clearly indicated by signals at δ1.46, 1.91–2.07, 2.39 ppm for two -CH_2 in addition to the signal at δ 3.32-3.67 for -OCH_2 in the tetrahydrofuran moiety [24, 25]. The substitution at position 2 was concluded from the signal at δ 3.9 ppm (1H, td, -$OCHCH=CHMe_2$). The presence of side chain-methyl butane-1-en-1-yl) in the position 2 of tetrahydronfuran was concluded by the two signals at δ 5.37 and 5.43 ppm assignable for two protons for each CH=CH in addition to the disubstituted methyls connected to a methine carbon ($CHMe_2$) which confirmed by a signal at δ 2.43 ppm. The presence of gem methyl was concluded from the signals at δ 1.62 and 1.64 ppm. Typically, 9 carbon signals were similar to those of 2-(3-Methyl butane-1-en-1-yl) tetrahydrofuran in the ^{13}C-NMR spectrum of compound (18-B) (1). Substitution at C-2 position was further deduced from the downfield location of C-2 (~ + 5 ppm) relative to that of tetrahydrofuran. The presence of CH=CH in the side chain-(methyl butane-1-en-1-yl) at C-2 was established from the signals at δ132.7, and 136.1 ppm, respectively. The identity of the gem methyls is due to the resonances at δ 16.4 and 29.3 ppm. The remaining carbon resonances of (18-B) were completely assigned by comparison with previously published corresponding data of structurally related compounds [24-27]. Therefore, compound 4 was finally identified as 2-(3-methyl butane -1-en-1-yl) tetrahydrofuran.

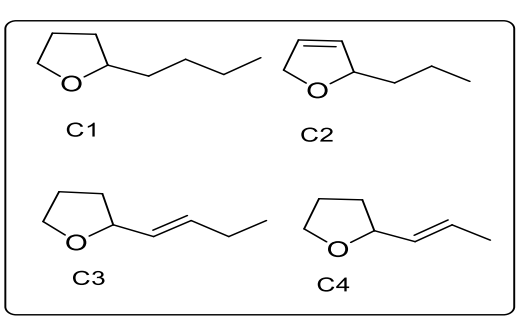

Fig. 1. Chemical structures of the identified compounds.

3.4. Biological evaluation

3.4.1. Antimicrobial activity

Table 2 explains how well two fungal sources, SA17 and SA18 yield both crude and refined compounds that are useful in killing bacteria. These fungal extracts have a variety of inhibitory qualities, each with its own distinct ingredients. The inhibition percentages for *S. aureus*, *E. coli*, *C. albicans*, *and A. niger* are displayed in the table.

The crude extract from the SA17 fungal source has strong antibacterial activity. It demonstrates a 50% inhibition of *S. aureus*, demonstrating a potent bactericidal impact. *Candida albicans* has a significant inhibition rate of 35%, indicating a noteworthy capacity to limit fungal growth. The inhibition of *A. niger* is somewhat reduced to 30.32%, although it remains statistically significant. The crude extract exhibits a very mild suppression of *E. coli* at a rate of 10.25%, indicating a selective microbial effect. In contrast, the pure compound 2 (C2) derived from SA17 does not exhibit any action against *S. aureus*, *C. albicans*, or *A. niger*, as shown by "NA" (not applicable) in the table. Nevertheless, it suppresses the growth of *E. coli* by 15.23%, indicating a distinct antibacterial impact on this gram-negative bacterium.

The SA17 purified compound (comp. 1) has antibacterial characteristics that are effective against a wide range of microorganisms. The results indicate a moderate level of inhibition against *S. aureus*, with a percentage of 15.10%. In contrast, there is a greater level of inhibition against *E. coli*, with a percentage of 30.12%. The activity of the substance against *C. albicans* is significant, reaching 45.6%, which suggests a robust antifungal effect. The inhibition of *A. niger* is reduced, specifically by 25.22%, indicating that the effectiveness varies when targeting various fungal strains. The wide-ranging effectiveness of Comp. 2 from SA17 makes it a very intriguing option for future exploration.

When analyzing the SA18 fungal source, we discover a similar pattern of mild antibacterial activity in its purified components. **C**3 has a modest level of activity, with a 10.02% inhibition of *S. aureus* and a 12% inhibition of *E. coli*. There is insufficient evidence about its effectiveness against *C. albicans* and *A. niger*, indicating either a lack of efficacy or unproven parameters. **C**4 has a modest level of antibacterial activity. It reduces the growth of *S. aureus* by 25.1% and *E. coli* by 16.2%. There is no evidence available about its effectiveness against *C. albicans* and *A. niger*, just like C3.

Compared to other samples, the SA17-crude extract exhibits the most potent antibacterial action, specifically against *S. aureus* and *C. albicans*. Out of all the pure compounds, C2 has notable inhibitory effects on all the microorganisms that were tested, except for *A. niger*, where its effectiveness is

somewhat diminished. The compounds C1 and those derived from SA18 have more selectivity and moderate antibacterial activities, indicating that specific bioactive components present in the crude extracts contribute to a wider range of activity.

The antimicrobial results showed that, the SA17 crude extract has a significant efficacy, particularly against *S. aureus* and *C. albicans*, with modest impact on *A. niger* and limited effectiveness against *E. coli*. On the other hand, C2 from SA17 demonstrating a significant activity against *E. coli*. Moreover, the SA18 extract exhibit diminished antibacterial efficacy and a higher degree of selectivity.

Table 2: Antimicrobial activity (%) of two fungus crude extracts and their purified compounds

Sample	Inhibition (%)			
	S. aureus	*E. coli*	*C. albicans*	*A. niger*
SA17-crude	50 ± 0.22	10.25 ± 0.12	35.00 ± 0.75	30.32 ± 2.35
C 1	15.10 ± 1.02	30.12 ± 0.29	45.6 ± 0.12	25.22 ± 0.15
C 2	NA	15.23 ± 0.12	NA	NA
SA18-crude	10.9 ± 0.22	22.21 ± 0.32	NA	NA
C3	10.02±0.13	12.0±0.109	NA	NA
C4	25.1 ± 1	16.2 ± 0.15	NA	NA

NA: Not active.

3.4.2. Acetylcholinesterase inhibition two fungus crude extracts and their purified compounds

The data presented in Table 3 reveal the acetylcholinesterase (AChE) inhibition potential of crude and purified compounds derived from two fungal sources, SA17 and SA18, across varying concentrations (50 µg, 100 µg, 200 µg, and 300 µg). The inhibitory percentages shed light on the varying efficacy of these extracts and their isolated constituents in curtailing AChE activity, an enzyme implicated in neurodegenerative ailments such as Alzheimer's disease [28-30].

For the SA17 fungal source, the crude extract manifests a concentration-dependent escalation in AChE inhibition. Specifically, at the lowest concentration of but progressively increasing inhibitory potential as the concentration rises. However, the purified 50 µg, the inhibition is recorded at 12.4%, which amplifies to 25% at 300 µg. This indicates that the crude extract holds a moderate compound 1 (C1) from SA17 displays no inhibition across all tested concentrations, suggesting that this particular compound does not contribute to AChE inhibition. In stark contrast, purified compound 2 **(**C2**)** from SA17 exhibits substantial inhibition, starting from 10.1% at 50 µg and reaching a significant 50.1% at 300 µg. This illustrates that Comp. 2 possesses a potent inhibitory effect, surpassing that of the crude extract. Examining the SA18 fungal source, a similar trend is observed with its crude extract, which shows a robust inhibitory effect starting at 25.9% at 50 µg and peaking at 51.2% at 300 µg. This crude extract thus demonstrates a strong and increasing potential to inhibit AChE. Meanwhile, (C3) from SA18, exhibits no inhibitory activity across all concentrations. However, C4 presents a milder inhibitory effect compared to C2, with inhibition percentages rising from 7.1% at 50 µg to 16.1% at 300 µg. This indicates a less pronounced but still notable inhibitory capability.

Table 3: Acetylcholinesterase inhibition (%) of two fungus crude extracts and their purified compounds

Sample	Acetylcholinesterase Inhibition (%)			
	50 µg	100 µg	200 µg	300 µg
SA17-crude	12.4 ± 1.23	15.7 ± 0.12	20.2 ± 2.02	25 ± 1.44
C 1	0.0	0.0	0.0	0.0
C 2	10.1 ± 1	20.2 ± 0.19	36.6 ± 0.2	50.1 ± 0.2
SA18-crude	25.9 ± 1.29	33.4 ± 1.37	46.8 ± 1.53	51.2 ± 1.36
C 3	0.0	0.0	0.0	0.0
C4	07.1 ± 1	10.2 ± 0.19	11.6 ± 0.2	16.1 ± 0.2
Ciprofloxacin (10µg/mL)	99.25±0.25	98.25±0.15	-	-

The inhibition of acetylcholinesterase (AChE) by crude and purified substances from fungal sources SA17 and SA18 was investigated at various doses. The SA17 crude extract has a moderate inhibition that is dependent on its concentration. However, its purified constituent C2 displays a potent inhibitory action which surpasses that of the crude extract. SA18's crude extract exhibits strong inhibition, whereas its refined component C4 has a moderate but significant impact. Both C1 from SA17 and C3 from SA18 do not contribute to the inhibition of AChE, highlighting the variety in the effectiveness of these compounds obtained from fungi.

3.5. *ADME-physiochemical properties*

The compound 2-pentyl tetrahydrohydrofuran which showed potent a good antimicrobial activity has been selected and studied for its ADME- physiochemical properties, with its a molecular weight of 142.24 g/mol, possesses a range of ADME physicochemical properties that suggest potential for pharmaceutical application. With ten heavy atoms and no aromatic heavy atoms, the compound exhibits a high degree of saturation, indicated by a fraction Csp3 of 1.00, suggesting a more flexible structure with four rotatable bonds. This flexibility can be advantageous for binding interactions in biological systems.

The compound features one hydrogen bond acceptor and no hydrogen bond donors, which may affect its solubility and permeability. The low Topological Polar Surface Area (TPSA) of 9.23 Å² typically correlates with favourable membrane permeability and oral bioavailability. This is supported by the compound's high gastrointestinal (GI) absorption and its ability to permeate the blood-brain barrier (BBB), suggesting potential central nervous system activity.

Lipophilicity, a critical factor in drug design, is represented by various log P values: iLOGP (2.77), XLOGP3 (2.97), WLOGP (2.75), MLOGP (2.15), SILICOS-IT (2.86), and a consensus log Po/w of 2.70. These values indicate moderate lipophilicity, which is optimal for membrane permeability without compromising aqueous solubility. The water solubility data, with log S values of -2.33 (ESOL), -2.83 (Ali), and -2.48 (SILICOS-IT), categorize the compound as soluble, albeit with varying solubility values (0.67 mg/ml to 0.47 mg/ml). This solubility range is adequate for oral administration (Fig. 2).

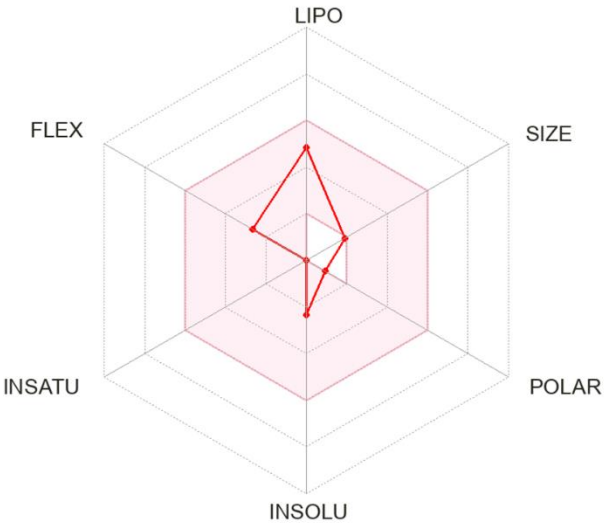

Fig. 2. Bioavailability radar chart.

Pharmacokinetically, the compound's high GI absorption and BBB permeability are notable, while its lack of interaction with P-glycoprotein (P-gp) (Fig. 3) and the enzymes known as cytochrome P450 (CYP) (CYP1A2, CYP2C19, CYP2C9, CYP2D6, CYP3A4) suggests minimal risk of drug-drug interactions and metabolic liabilities. The skin permeation coefficient (Log Kp) of -5.06 cm/s indicates low transdermal absorption, limiting its suitability for topical applications (Table 4).

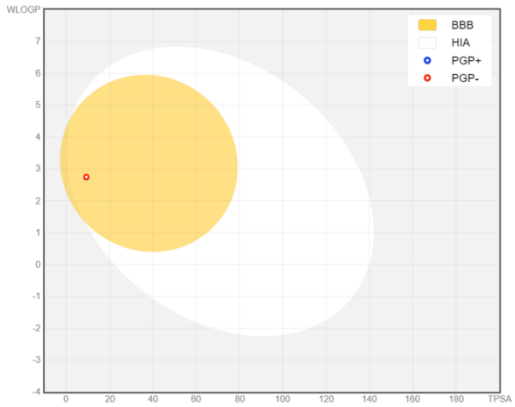

Fig. 3. Diagram of bioled eggs. The BOILED-Egg layout of Hyscion. The white region (GI) indicates a very high probability of HIA (GI) absorption, while the yellow zone (yolk) indicates a very possible BBB permeability. The outside grey area represents molecules with no brain penetration and minimal absorption. Additionally, the points are coloured red if the P-GP non-substrate (PGP) is projected and blue if the P-gp substrate (PGP+) is anticipated

Table 4: Pharmacokinetics properties of 2-pentyl tetrahydrohydrofuran

Pharmacokinetics	
GI absorption	High
BBB permeant	Yes
P-gp substrate	No
CYP1A2 inhibitor	No
CYP2C19 inhibitor	No
CYP2C9 inhibitor	No
CYP2D6 inhibitor	No
CYP3A4 inhibitor	No
Log K_p (skin permeation)	-5.06 cm/s

From a druglikeness perspective, the compound adheres to Lipinski's rule of five with no violations, supporting its potential as an orally active drug. The compound meets the criteria of Veber and Egan filters, further endorsing its druglikeness. However, it fails the Ghose filter due to its low molecular weight (<160) and the Muegge filter due to violations related to molecular weight and heteroatom count. Despite these violations, the bioavailability score of 0.55 is encouraging for oral administration.

In medicinal chemistry assessments, the compound shows no PAINS or Brenk alerts, suggesting a low likelihood of problematic reactive functionalities. The synthetic accessibility score of 2.53 indicates that the compound can be synthesized with relative ease. However, the leadlikeness criterion is not fully met due to its low molecular weight (<250), which may necessitate structural optimization to enhance its therapeutic potential.

Conclusion

The findings of this research underscore the rich potential of marine-derived endophytic fungi as sources of bioactive metabolites with varied medical applications. Two fungal strains, *Aspergillus* sp. SA17 and *Aspergillus* sp. SA18, isolated from the Red Sea, produced four structurally distinct compounds with varying degrees of antimicrobial and acetylcholinesterase inhibitory activities. The SA17 crude extract, particularly its C2 compound, demonstrated significant antimicrobial efficacy and potent acetylcholinesterase inhibition, surpassing the effects of the crude extract. Meanwhile, SA18 showed selective antibacterial activity, with its C4 compound offering moderate inhibition. Some of the obtained compounds displayed anti- acetylcholinesterase inhibition activities. ADME characteristics are important for drug development since they establish the medication's safety and efficacy in the body. These results highlight the diverse bioactivities of fungal metabolites and their potential as candidates for therapeutic development.

Abbreviations

ADME: Absorption, Distribution, Metabolism, and Excretion; **AChE**: Acetylcholinesterase; **SCUBA**: Self-Contained Underwater Breathing Apparatus; **PDA**: Potato Dextrose Agar; **18S rRNA**: 18S Ribosomal Ribonucleic acid; **DNA**: Deoxyribonucleic acid; **PCR**: Polymerase chain Reaction; **NCBI**: National Centre for Biotechnology Information; **BLAST**: Basic Local Alignment Search Tool; **MEGA7**: Molecular Evolutionary Genetics Analysis; **TLC**: Thin Layer Chromatography; $\mathbf{R}_f$: Retention Factor; **DTNB**: 5,5-DiThio-bis-(2-NitroBenzoic acid); ^{1}**H-NMR**: Proton Nuclear Magnetic Resonance; ^{13}**C-NMR**: Carbon-13 Nuclear Magnetic Resonance; **MHz**: Megahertz; **CD_3OD**: Deuterated Methanol; **TPSA**: Topological Polar Surface Area; **GI**: Gastrointestinal; BBB: Blood-Brain Barrier; **P-gp**: P-glycoprotein.

References

[1] Qader MM, Hamed AA, Soldatou S, Abdelraof M, Elawady ME, Hassane ASI, Belbahri L, Ebel R, Rateb ME. Antimicrobial and antibiofilm activities of the fungal metabolites isolated from the marine endophytes *Epicoccum nigrum* M13 and *Alternaria alternata* 13A. *Mar. Drugs*. 2021; 19: 232.

[2] Adeleke BS, Olubukola OP, Bernard RG. Plant growth promoting root-colonizing bacterial endophytes. *Rhizosphere*. 2021; 20: 100433.

[3] Ginsburg O, Bray F, Coleman MP, Vanderpuye V, Eniu A, Kotha SR, Sarker M, Huong TT, Allemani C, Dvaladze A, et al. The global burden of women's cancers: A grand challenge in global health. *Lancet*. 2017; 389: 847-860.

[4] Strobel G, Daisy B, Castillo U, Harper J. Natural products from endophytic microorganisms. *J. Nat. Prod.* 2004; 67: 257-268.

[5] Du L, Li X, Su X, Wang C, Guo Y, Wu J. Aspergiolide A, a novel compound from a marine-derived fungus, *Aspergillus versicolor*. *Mar. Drugs*. 2014; 12: 220-228.

[6] Wu J, He Y, Yang B, Liu L. Versicolactones and their bioactivity from the mangrove endophytic fungus *Aspergillus versicolor*. *Fitoterapia*. 2013; 91: 14-20.

[7] Liu Z, Zhang Q, Peng X, Li W. Sydonic acids A and B, two new isocoumarins from the marine-derived fungus *Aspergillus sydowii*. *Nat. Prod. Res.* 2019; 33: 2329-2334.

[8] Li L, Li D, Luan Y, Guo L, Yang S. Antioxidant and cytotoxic activities of sydowic acid and other metabolites from the marine-derived fungus *Aspergillus sydowii*. *Molecules*. 2017; 22: 969.

[9] Kim YS, Kim SK, Park SJ. Apoptotic effect of demethoxyfumitremorgin C from marine fungus *Aspergillus fumigatus* on PC3 human prostate cancer cells. *Chem. Biol. Interact.* 2017; 269: 18-24.

[10] Abdel-Aziz MS, Ghareeb MA, Saad AM, Refahy LA, Hamed AA. Chromatographic isolation and structural elucidation of secondary metabolites from the soil-inhabiting fungus *Aspergillus fumigatus* 3T-EGY. *Acta Chromatogr.* 2018; 30, 243-249.

[11] El-khouly HI, Hamed AA, El-Hosainy AM, Ghareeb MA, Sidkey NM. Bioactive secondary metabolite from endophytic *Aspergillus tubenginses* ASH4 isolated from *Hyoscyamus muticus*: Antimicrobial, antibiofilm, antioxidant, and anticancer activity. *Pharmacogn. J.* 2021; 13: 434-442.

[12] Hamed AA, Soldatou S, Qader MM, Arjunan S, Miranda KJ, Casolari F, Pavesi C, Diyaolu OA, Thissera B, Eshelli M, et al. Screening fungal endophytes derived from under-explored Egyptian marine habitats for antimicrobial and antioxidant properties in factionalized textiles. *Microorganisms*. 2020; 8: 1617.

[13] El-Neekety AA, Abdel-Aziz MS, Hathout AS, Hamed AA, Sabry BA, Ghareeb MA, Aly SE, Abdel-Wahhab MA. Molecular identification of newly isolated non-toxigenic fungal strains having antiaflatoxigenic, antimicrobial, and antioxidant activities. *Der Pharma Chem.* 2016; 8: 121-134.

[14] Abdelgawad MA, Hamed AA, Nayl AA, Badawy MSEM, Ghoneim MM, Sayed AM, Hassan HM, Gamaleldin NM. The chemical profiling, docking study, and antimicrobial and antibiofilm activities of

the endophytic fungi *Aspergillus* sp.AP5. *Molecules*. 2022; 27: 1704.

[15] Lu JJ, Chen CH, Bartlett MS, Smith JW, Le CH. Comparison of six different PCR methods for detection of *Pneumocystis carinii*. *J. Clin. Microbiol.* 1995; 33: 2785-2788.

[16] Khazaal AQ, Haque N, Krager CR, Krager SL, Chambers C, Wilber A, Tischkau SA. Aryl hydrocarbon receptor affects circadian-regulated lipolysis through an E-Box-dependent mechanism. *Mol. Cell. Endocrinol.* 2023; 559: 111809.

[17] Elawady ME, Hamed AA, Alsallami WM, Gabr EZ, Abdel-Monem MO, Hassan MG. Bioactive metabolite from endophytic *Aspergillus versicolor* SB5 with anti-acetylcholinesterase, anti-Inflammatory, and antioxidant activities: *In vitro* and *in silico*. *Microorganisms*. 2023; 11: 1062.

[18] El-Hosari D, Abdou M, Abdel-Razek AS, Hamed AA, Shaaban M, El-Gindi M. Preliminary investigation of the fungal endophytic extract isolated from *Tabernaemontana pandacaqui* leaves and evaluation of its antioxidant and cytotoxic potentials. *J. Adv. Pharm. Res.* 2022; 6: 68-77.

[19] Alhadrami HA, Orfali R, Hamed AA, Ghoneim MM, Hassan HM, Hassane ASI, Rateb ME, Sayed AM, Gamaleldin NM. Flavonoid-coated gold nanoparticles as efficient antibiotics against gram-negative bacteria-Evidence from *in silico*-supported *in vitro* studies. *Antibiotics*. 2021; 10: 968.

[20] Ingkaninan K. Temkitthawon P, Chuenchom K, Yuyaem T, Thongnoi W. Screening for acetylcholinesterase inhibitory activity in plants used in Thai traditional rejuvenating and neurotonic remedies. *J. Ethnopharmacol.* 2003; 89: 261-264.

[21] McPhee S, Hodges LD, Wright PFA, Wynne PM, Kalafatis N, Harney DW, Macrides TA. Anti-cyclooxygenase Effects of Lipid Extracts from the New Zealand .Green-Lipped Mussel, *Perna canaliculus*. *Comp. Biochem. Physiol. Part B Biochem. Mol. Biol.* 2007; 146: 346-356.

[22] Hussein ME, Mohamed OG, El-Fishawy AM, El-Askary HI, Hamed AA, Abdel-Aziz MM, Alnajjar R, Belal A, Naglah AM, Almehizia AA, et al. Anticholinesterase activity of Budmunchiamine alkaloids revealed by comparative chemical profiling of two *Albizia* spp., molecular docking and dynamic studies. *Plants*. 2022; 11: 3286.

[23] Noble A, McCarver SJ, MacMillan DWC. Merging photoredox and nickel catalysis: Decarboxylative cross-coupling of carboxylic acids with vinyl halides. *J. Am. Chem. Soc*. 2015; 137: 624-627.

[24] Louie J, Bielawski CW, Grubbs RH. Tandem Catalysis: The sequential mediation of olefin metathesis, hydrogenation, and hydrogen transfer with single-component Ru complexes, *J. Am. Chem. Soc*. 2001; 123: 11312-11313.

[25] Babij NR, McCusker EO, Whiteker GT, Canturk B, Choy N , Creemer LC, De Amicis CV, Hewlett NM, Johnson PL, Knobelsdorf JA, Li F, Lorsbach BA, Nugent BM, Ryan SR, Smith MR, Yang Q. NMR chemical shifts of trace impurities: Industrially preferred solvents used in process and green chemistry. *Org. Process Res. Dev*. 2016; 20: 661-667.

[26] Cheng X, Quintanilla CD, Zhang L. Total synthesis and structure revision of diplobifuranylone B. *J. Org. Chem*. 2019; 84: 11054-11060.

[27] Zhou L, Cao X, Yang C, Wu X, Zhang L. Endophytic fungi of *Paris polyphylla* var. yunnanensis and steroid analysis in the fungi. *Nat. Prod. Res. Dev*. 2004; 16: 198200.

[28] Cummings J, Rabinovici GD, Atri A, Aisen P, Apostolova LG, Hendrix S, et al. Aducanumab: appropriate use *recommendations* update. *J. Prev. Alzheimers Dis*. 2022; 9: 221-230.

[29] van Dyck CH, Swanson CJ, Aisen P, Bateman RJ, Chen C, Gee M, et al. Lecanemab in early Alzheimer's disease. *N. Engl. J. Med*. 2023; 388:9-21.

[30] Budd Haeberlein S, Aisen PS, Barkhof F, Chalkias S, Chen T, Cohen S, et al. Two randomized phase 3 studies of aducanumab in early Alzheimer's disease. *J. Prev. Alzheimers Dis*. 2022; 9:197-210.